ADVANCED MATERIALS

www.advmat.de

# Encoding Random Hot Spots of a Volume Gold Nanorod Assembly for Ultralow Energy Memory

*Qiaofeng Dai, Min Ouyang, Weiguang Yuan, Jinxiang Li, Banghong Guo, Sheng Lan,* Songhao Liu, Qiming Zhang, Guang Lu, Shaolong Tie,* Haidong Deng, Yi Xu, and Min Gu**

**Data storage with ultrahigh density, ultralow energy, high security, and long lifetime is highly desirable in the 21st century and optical data storage is considered as the most promising way to meet the challenge of storing big data. Plasmonic coupling in regularly arranged metallic nanoparticles has demonstrated its superior properties in various applications due to the generation of hot spots. Here, the discovery of the polarization and spectrum sensitivity of random hot spots generated in a volume gold nanorod assembly is reported. It is demonstrated that the two-photon-induced absorption and two-photon-induced luminescence of the gold nanorods adjacent to such hot spots are enhanced significantly because of plasmonic coupling. The polarization, wavelength, and spatial multiplexing of the hot spots can be realized by using an ultralow energy of only a few picojoule per pulse, which is two orders of magnitude lower than the value in the state-of-the-art technology that utilizes isolated gold nanorods. The ultralow recording energy reduces the cross-talk between different recording channels and makes it possible to realize rewriting function, improving significantly both the quality and capacity of optical data storage. It is anticipated that the demonstrated technology can facilitate the development of multidimensional optical data storage for a greener future.**

Twenty-first century is an era of big data that requires information generation, transmission, and storage with ultralow energy consumption.[1] Plasmonic systems composed of metallic nanoparticles or nanostructures are considered as one of the most promising platforms on which information generation, transmission, and storage with ultralow energy can be realized and integrated. In a plasmonic system, the strongly localized modes with significantly enhanced electromagnetic field are generally referred to as hot spots. So far, plasmonic coupling in metallic nanoparticle assemblies of regular spatial arrangements has demonstrated its superior properties in digital information processing,[2] super-resolution imaging,[3] and solar cells[4] due to the generation of hot spots. As a promising way to meet the challenge of storing big data,[1] optical data storage by exploiting the interaction between laser and metallic nanoparticles[5–18] has attracted great interest and

Prof. Q. Dai, Dr. M. Ouyang, W. Yuan, J. Li, Prof. B. Guo, Prof. S. Lan, Prof. S. Liu
Guangdong Provincial Key Laboratory of Nanophotonic Functional Materials and Devices
School of Information and Optoelectronic Science and Engineering
South China Normal University
Guangzhou 510006, P. R. China
E-mail: slan@scnu.edu.cn

Dr. Q. Zhang, Prof. M. Gu
Centre for Micro-Photonics and Ultrahigh Bandwidth Devices for Optical Systems
Faculty of Science
Engineering and Technology
Swinburne University of Technology
Hawthorn, Victoria 3122, Australia
E-mail: min.gu@rmit.edu.au

G. Lu, Prof. S. Tie
School of Chemistry and Environment
South China Normal University
Guangzhou 510006, P. R. China
E-mail: tiesl@scnu.edu.cn

Prof. H. Deng
College of Science
South China Agricultural University
Guangzhou 510642, P. R. China

Prof. Y. Xu
Department of Electronic Engineering
College of Information Science and Technology
Jinan University
Guangzhou 510632, P. R. China

Prof. M. Gu
Artificial-Intelligence Nanophotonics Laboratory
School of Science
RMIT University
Melbourne, VIC 3001, Australia

**DOI: 10.1002/adma.201701918**

5D optical data storage by utilizing the polarization- and wavelength-dependent two-photon-induced luminescence (TPL) of individual gold nanorods (GNRs) has been demonstrated.[6]

Basically, hot spots are known to exist at the intersections between plasmonic structures such as the gap of a GNR antenna. The plasmonic coupling in GNR dimers has been studied with the focus on the modification in the linear extinction spectra.[19,20] In addition, the effects of coupling on the two-photon-induced absorption (TPA) and TPL of GNR antennas were also examined.[21–23] In a volume GNR assembly, there exist randomly distributed hot spots induced by the plasmonic coupling between GNRs if the volume density of GNRs is large enough (**Figure 1**a–d). In particular, such hot spots depend strongly on the polarization and wavelength of the excitation laser (Figure 1a–d), implying the possibility for polarization and wavelength multiplexing. Although the density of hot spots is much lower than that of GNRs, the existence of hot spots significantly enhances the TPA and TPL of the adjacent GNRs, which dominate the TPA and TPL of the GNR assembly. Moreover, such hot spots are quite sensitive to the gap widths between GNRs and small deformations of the adjacent GNRs may result in the disappearance of the hot spots and the dramatic reduction in the TPL of the GNR assembly. All these features imply that the encoding of random hot spots can be exploited to realize optical memory with ultralow energy and ultrahigh density.

Here, we report on the discovery of the polarization and spectrum sensitivity of random hot spots in a volume GNR assembly. We demonstrate that the TPA and TPL of the GNRs adjacent to hot spots are enhanced significantly because of plasmonic coupling. The polarization and wavelength multiplexing of hot spots and multilayer data storage can be realized by using an ultralow energy of only a few picojoule (pJ) per pulse, which has been reduced by nearly two orders of magnitude compared with the state-of-the-art technology that utilizes isolated GNRs.[5–7] The ultralow recording energy reduces the cross-talk between different recording channels and makes it possible to realize rewriting function, improving significantly both the quality and capacity of optical data storage.

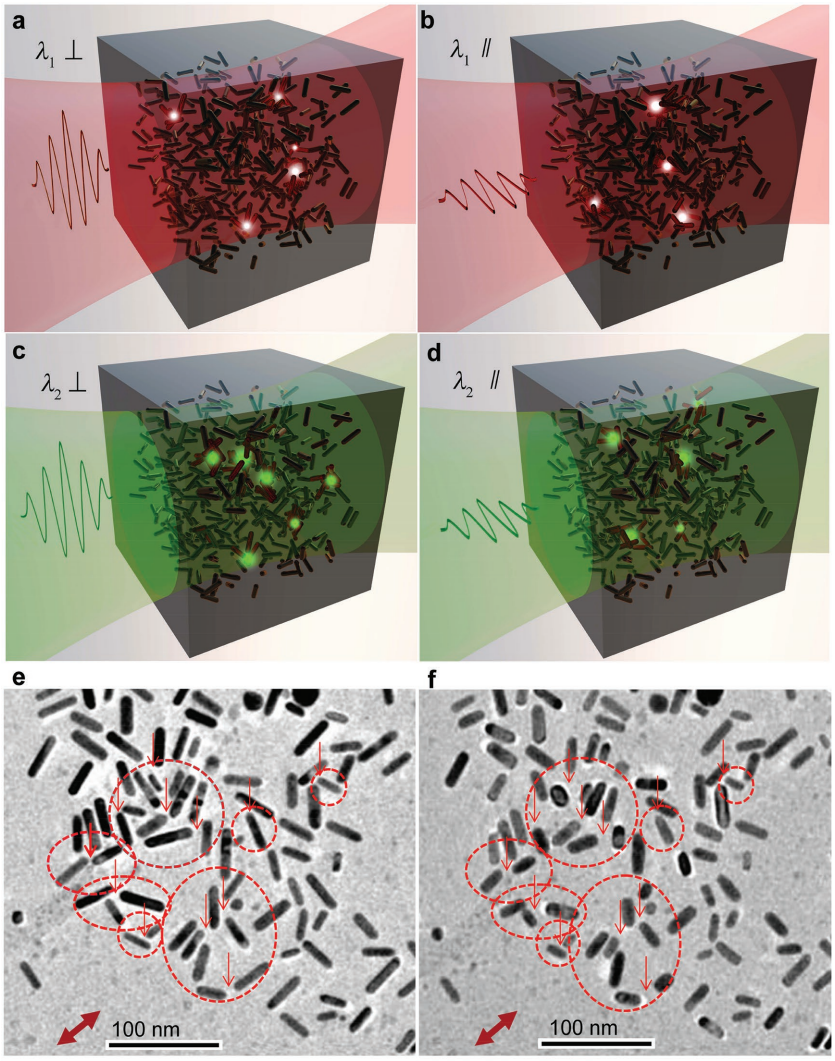


**Figure 1.** a–d) Schematics showing the polarization and wavelength-sensitive hot spots created in a volume GNR assembly through the plasmonic coupling of GNRs. e,f) TEM images of the GNR assembly before and after the irradiation of fs laser pulses with a pulse energy of ≈8.23 pJ (or fluence of ≈0.50 mJ cm$^{-2}$) and an irradiation time of 20 ms. The expected hot spots are indicated by arrows while the deformed GNRs around the hot spots are enclosed by dashed circles or ellipses. The laser polarization is indicated by the thick arrow.

The response of the hot spots created in a simple GNR assembly to femtosecond (fs) laser pulses was examined by comparing the transmission electron microscopy (TEM) images of the GNR assembly before and after the irradiation of fs laser pulses (Figure 1e,f). The GNRs with an average diameter of ≈8 nm and an average length of ≈34 nm were synthesized by using a modified seedless method.[24] The pulse energy (or fluence) and the exposure time were deliberately chosen to be ≈8.23 pJ (≈0.50 mJ cm$^{-2}$) and 20 ms so that the GNRs adjacent to the hot spots were deformed. By comparing the two images, one can easily identify the hot spots (Figure 1e,f) whose positions are in good agreement with those revealed by the numerical simulation (Figure S1a, Supporting Information). After examining a large number of 2D GNR assemblies, it was found that the pulse energy (or fluence) for melting only the GNRs around the hot spots can be further reduced to be ≈4 ± 0.4 pJ (≈0.25 ± 0.025 mJ cm$^{-2}$) (Figure S1c–f, Supporting Information). It was found that the melting or deformation of GNRs appeared mainly at the vicinities of the hot spots and it was no longer determined by the orientation and aspect ratio of GNRs as in the uncoupled case. These results demonstrate that it is feasible to encode the random hot spots in a volume GNR assembly by using fs laser pulses with ultralow energy.

In optical data storage, the quality of a recorded pattern is usually characterized by the correlation coefficient ($C$) and contrast ($R$) which can be improved by increasing the recording energy (Figure S2, Supporting Information). However, the cross-talk between different recording channels becomes larger with increasing the recording energy (Figures S3–S5, Supporting Information), leading to the reduction of storage capacity and possibly the damage of storage media.[5] Therefore, how to reduce the recording energy has become a big challenge in order to fully exploit the multiplexing function. Intuitively, the recording energy can be reduced by using small GNRs because the melting energy of a GNR is proportional to its mass.[25] In addition, the melting point of gold nanoparticles (GNPs) drops exponentially when the diameter of GNPs becomes smaller than 5 nm.[26] Although small GNRs are demonstrated to possess higher efficiency for optic-thermal conversion,[27,28] they may exhibit larger deformation threshold due to better thermal coupling and faster heat dissipation to the environment.[29] Therefore, simply replacing the large GNRs in storage media with small ones did not render a decrease of the recording energy because the absorption cross section of a GNR also scales with its volume.[30]

The nonlinear optical properties of the GNRs around the hot spots, which are expected to be modified significantly, were first investigated by numerical simulations based on the finite-difference time-domain (FDTD) method. The TPA of a GNR is proportional to the integration of $|E|^4$ over the volume of the GNR and the total TPA of a GNR array can be obtained by summing up the contributions of all the GNRs, as established previously.[31–33] We plot the dependence of the normalized TPL of a single GNR on the polarization angle ($\alpha$) which follows a function of $\cos^4\alpha$[34] (**Figure 2**a). Since it describes the relative contributions of the GNRs with different polarization angles in a recording unit, the total TPL intensity of the recording unit is given by $\int_0^{\pi/2}\cos^4\alpha \mathrm{d}\alpha$ for the uncoupled case. In data recording, one needs to melt the GNRs with $0° < \alpha < \beta$ in order to achieve a contrast to represent an information unit of "0," where $\beta$ is the maximum polarization angle of the melted GNRs (Figure 2a). However, the melting of these GNRs will lead to a cross-talk at other polarization angles (e.g., $\alpha = 60°$) and inhibit the polarization multiplexing in this direction if it is large. An improvement can be achieved by modifying the above relationship to a steeper function such as $\cos^8\alpha$ and it can be realized by utilizing hot spots (Figures S6 and S7, Supporting Information). The physical model used to study the effects of hot spots is a GNR array composed of $10 \times 10$ randomly oriented GNRs arranged on a square lattice with a lattice constant of $S$. The coupling strength between GNRs can be adjusted by varying the value of $S$. The normalized linear absorption spectra were calculated for different GNR arrays where a significant broadening of the absorption spectrum with decreasing lattice constant is observed (Figure 2b), in good agreement with the experimental observations. The linear absorption of a GNR at a certain wavelength is equal to the integration of $\kappa|E|^2$ over the GNR volume, where $\kappa$ is the imaginary part of the complex refractive index of gold. We also calculated the normalized nonlinear optical absorption spectra which characterize the TPA of the GNR arrays (Figure 2b). For the GNR array with strong coupling ($S = L$), the linear and nonlinear absorption peaks are widely separated. This feature is completely different from the GNR array without coupling ($S = 3L$) in which the two peaks coincide.

We present the distributions of $|E|^4$ for the two GNR arrays which reflect the TPA or TPL of individual GNRs[31–33] (Figure 2c,d). In the array with $S = 3L$, the TPL of individual GNRs is determined mainly by the corresponding polarization angle. With increasing coupling, the brightest GNR is changed and the TPL is governed by hot spots. It is found that the TPA of the brightest GNR is enhanced by a factor of ≈25 owing to the existence of the hot spot and the melting of this GNR leads to a large contrast of ≈0.32. In the array with $S = 3L$, the ratio of the TPL of the brightest GNR to the total TPL is only 3.16%. Surprisingly, this value is increased dramatically to ≈48.1% in the array with $S = L$. Although the area of the array with $S = L$ is only about one-ninth of that of the array with $S = 3L$, the total TPA is enhanced by a factor of ≈1.87, implying that it can harvest more energy from the irradiated laser light. In addition, the enhanced heat accumulation effect together with the large volume density of heat sources will generate a much higher temperature which in turn leads to a dramatic reduction in recording energy (Figures S8 and S9, Supporting Information).

We calculated the normalized TPL intensity distributions for different GNR arrays and also for different excitation wavelengths (Figure 2e). Assuming that the orientations of GNRs in all GNR arrays are uniformly distributed in [0°, 90°], a correlation between the number of GNRs and the polarization angle can be established. For the array with $S = 3L$, a distribution close to $\cos^4\alpha$ is observed. With increasing coupling, the contrast between the bright and dark GNRs is enlarged, which leads to a function much steeper than $\cos^4\alpha$. This behavior becomes more pronounced at long excitation wavelengths. We also calculated the evolution of the nonlinear absorption spectrum for the array with $S = L$ when GNRs are melted sequentially into nanospheres (Figure 2f). The melting of the brightest GNR results in a contrast of ≈0.32 at 1070 nm and the TPL of the array remains unchanged for wavelengths shorter than 1020 nm, which implies that one can use 1020 nm as the second wavelength for data recording. A contrast as large as ≈0.97 is obtained if the second brightest GNR is also melted. In this case, a wavelength separation of ≈70 nm (at 1000 nm) is sufficient for wavelength multiplexing.

In order to confirm the effects of hot spots on the optical data storage predicted by the numerical simulations, we fabricated polyvinyl alcohol (PVA) films doped with small GNRs of different volume densities as storage media (Figure S10, Supporting Information). Here, we show the TEM images for the GNRs distributed in air and PVA films (**Figure 3**a,b). The GNRs dispersed in the PVA film appear to be vague because PVA is an insulator. The coupling strength between GNRs was simply controlled by adjusting the volume density of GNRs. With increasing the volume density of GNRs, a significant broadening of the extinction spectrum was observed (Figure S10c, Supporting Information). As an example, we show two patterns recorded and extracted by using the two polarization states of the laser (0° and 90°) (Figure 3c,d). The high-quality data storage with $C > 0.93$ and $R > 0.61$ (Figure 3e,f) was realized by using a recording energy (or fluence) as low as 3.29 pJ (0.20 mJ cm$^{-2}$), which has been reduced by nearly two orders of magnitude as compared with the state-of-the-art technology.[5–7] Further

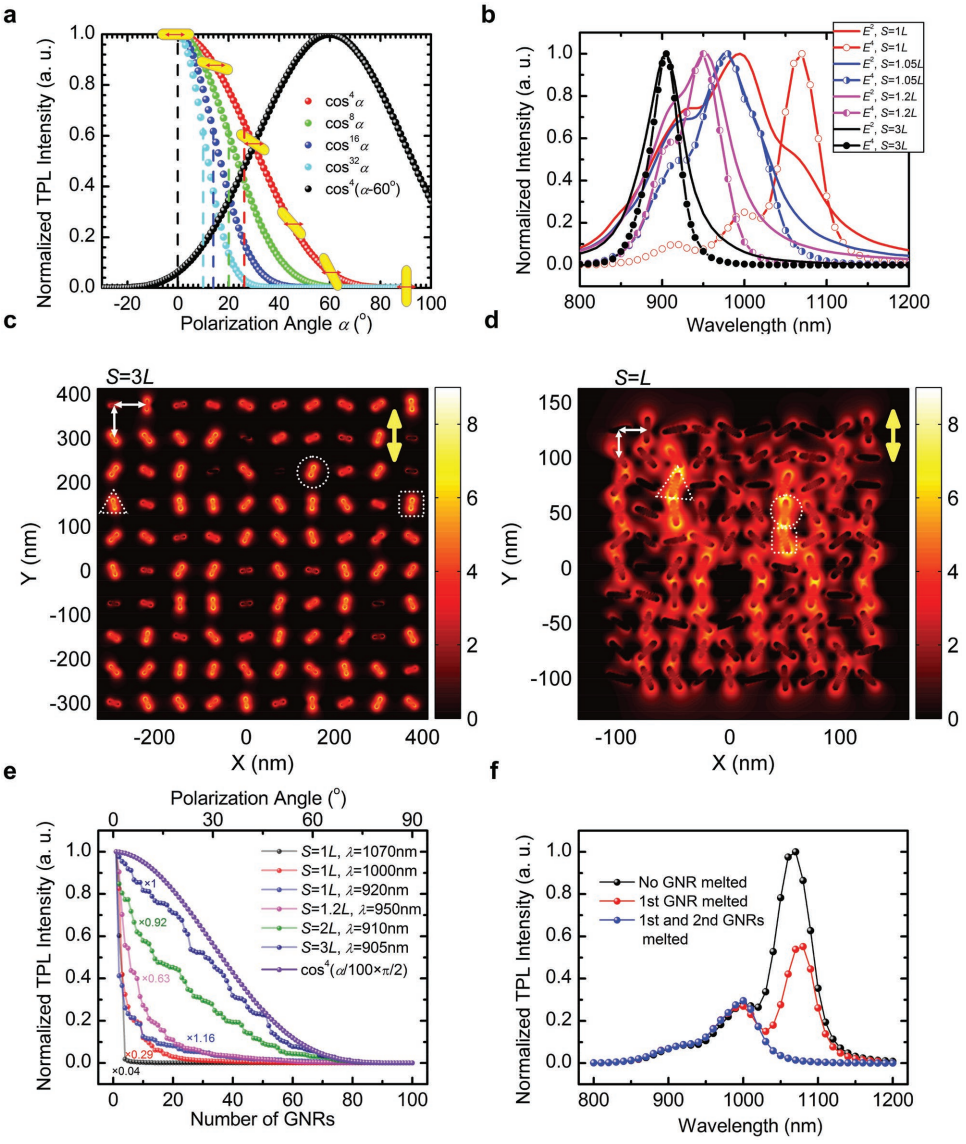


**Figure 2.** a) Dependence of the normalized TPL intensity of a GNR on the polarization angle which follows a function of $\cos^4\alpha$. It also represents the relative contributions of GNRs with different polarization angles to the total TPL intensity of a recording unit when the polarization of the fs laser light is chosen to be $\alpha = 0°$. Similar relationship when the polarization of the fs laser light is chosen to be $\alpha = 60°$ is also presented. The red dashed line indicates that the melting of GNRs with $0° < \alpha < 25°$ is necessary in order to achieve a contrast of 0.50. Other relationships between the TPL intensity and the polarization angle described by steeper functions of $\cos^8\alpha$, $\cos^{16}\alpha$, and $\cos^{32}\alpha$ are plotted and the color dashed lines indicate the maximum polarization angles for the melted GNRs when a contrast of 0.50 is required. b) Normalized linear and nonlinear absorption spectra calculated for GNR arrays with different lattice constants ranging from $3L$ to $L$. c,d) Distribution of $|E|^4$, which represents the TPA or TPL of GNRs, calculated for GNR arrays with $S = 3L$ and $S = L$ for vertically polarized excitation at 905 and 1070 nm, respectively. In each case, the GNRs with the top three TPA or TPL are enclosed by dashed circle (first), square (second), and triangle (third). e) Normalized TPL intensity distributions with descending order calculated for GNR arrays with different lattice constants and also for the GNR array with $S = L$ at different wavelengths. f) Evolution of the nonlinear absorption spectrum for the GNR array with $S = L$ when the GNR with the largest TPA is melted or the first two GNRs with the largest TPA are melted.

reduction in recording energy is expected for a longer excitation wavelength (Figure 2f). In addition, neither cross-talk nor morphology change was observed on the storage film after data recording (Figure S11, Supporting Information).

In order to verify the improvement of polarization multiplexing achieved by using random hot spots, we performed data recording at three polarization states of 0°, 60°, and 120° and obtained high-quality patterns with $C > 0.99$ and $R > 0.60$ (**Figure 4**a–c). No cross-talk was observed. This feature verifies that polarization multiplexing is benefited from both the low recording energy and the modified nonlinear optical responses. In fact, the realization of high-quality data storage at four polarization states (0°, 45°, 90°, and 135°) (Figure S12, Supporting Information), which cannot be achieved by using uncoupled GNRs (Figure S13, Supporting Information), was also demonstrated. Apart from the advantage in polarization multiplexing, the low recording energy is also helpful for wavelength multiplexing. As mentioned above, the coupling of GNRs results in

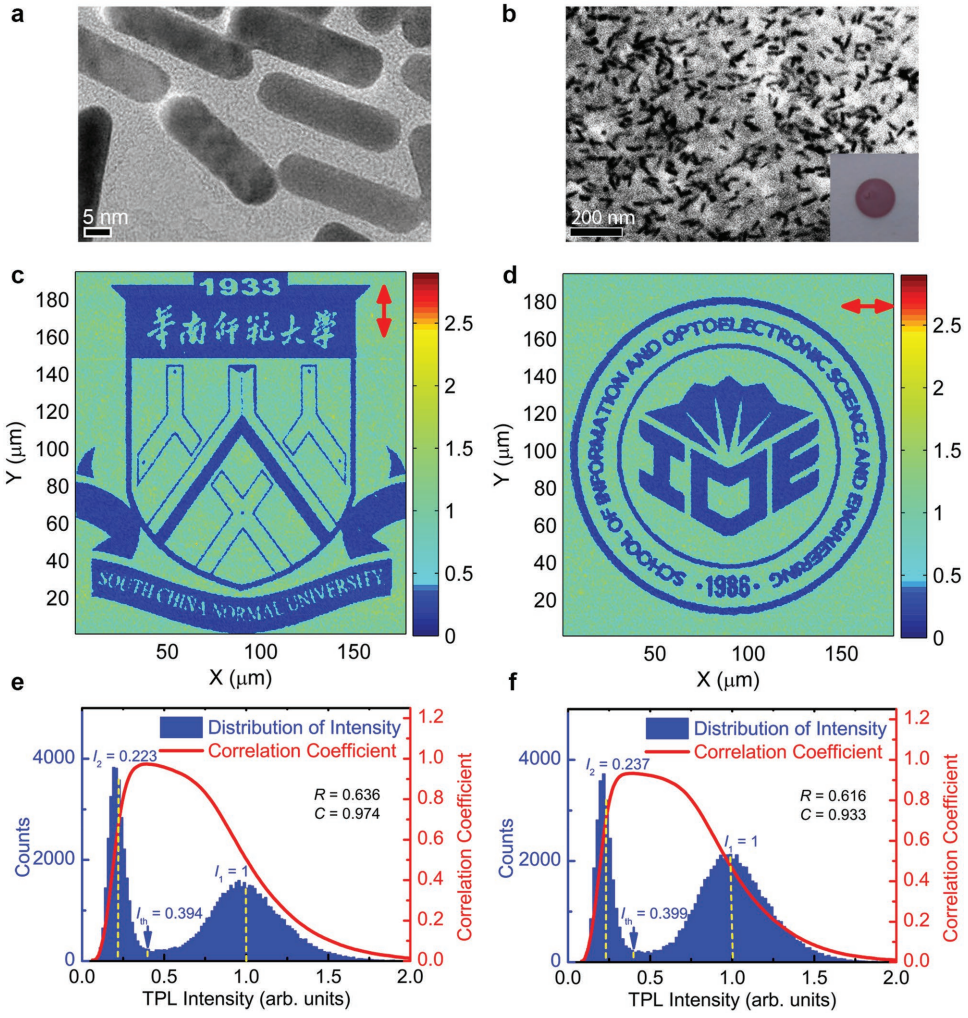


**Figure 3.** a,b) TEM images for small GNRs dispersed in air and in a PVA film. The photo for a typical GNR-PVA film is also provided (see the inset of (b)). c,d) Patterns recorded in a GNR-PVA film with a volume density of ≈800 GNR $\mu m^{-3}$ by using vertically and horizontally polarized fs laser light at 750 nm and extracted by detecting the TPL intensities of all the information units with fs laser light of the same polarization and wavelength. They are the LOGOs of the South China Normal University (SCNU) and the School of Information of Optoelectronic Science and Engineering of SCNU, respectively. The pulse energies (or fluences) used for data recording and readout were 3.29 and 0.53 pJ (0.20 and 0.033 mJ $cm^{-2}$), respectively. e,f) Distribution of the TPL intensities of all information units and the calculated correlation coefficients and contrasts for the patterns shown in (c) and (d).

a significant broadening of the extinction spectra which can be exploited for wavelength multiplexing. Since hot spots are used for optical memory, the uniformity of GNRs is no longer important, as demonstrated in the storage medium prepared by mixing GNRs with different aspect ratios (Figure S14, Supporting Information). We examined the data recording at two wavelengths separated by 40 nm and found no cross-talk (Figure S15, Supporting Information). The data recording at two wavelengths of 800 and 750 nm by utilizing two and four polarization states was also demonstrated (Figures S16 and S17, Supporting Information). This feature implies that the number of wavelength channels can be increased significantly and the fabrication tolerance of the storage media is enlarged. By lowering the recording energy, we also found that the lateral size of information units could be reduced to 0.50 × 0.50 $\mu m^2$ with negligible cross-talk (Figure S18, Supporting Information). Benefiting from the low recording energy, the separation between the two neighboring storage layers without cross-talk was reduced to be ≈4.0 μm and no spacer layer was needed (Figure 4d–h). Previously, a 10 μm thick transparent spacer layer was used between the two neighboring layers for thermal isolation.[6] As a result, the total number of storage layers available in a 1 mm thick disk can be increased to ≈250.

As the most important application of low recording energy, we demonstrated the possibility of rewriting the storage medium which relies on the modified TPL distribution induced by hot spots (see Figure 2e). As demonstrated numerically and experimentally, the number of melted GNRs necessary for achieving a target contrast is reduced significantly by hot spots. As a result, the GNRs in an information unit, which are simulated by using a GNR array composed of 10 × 10 GNRs (see the inset of **Figure 5**a), can be classified into several groups

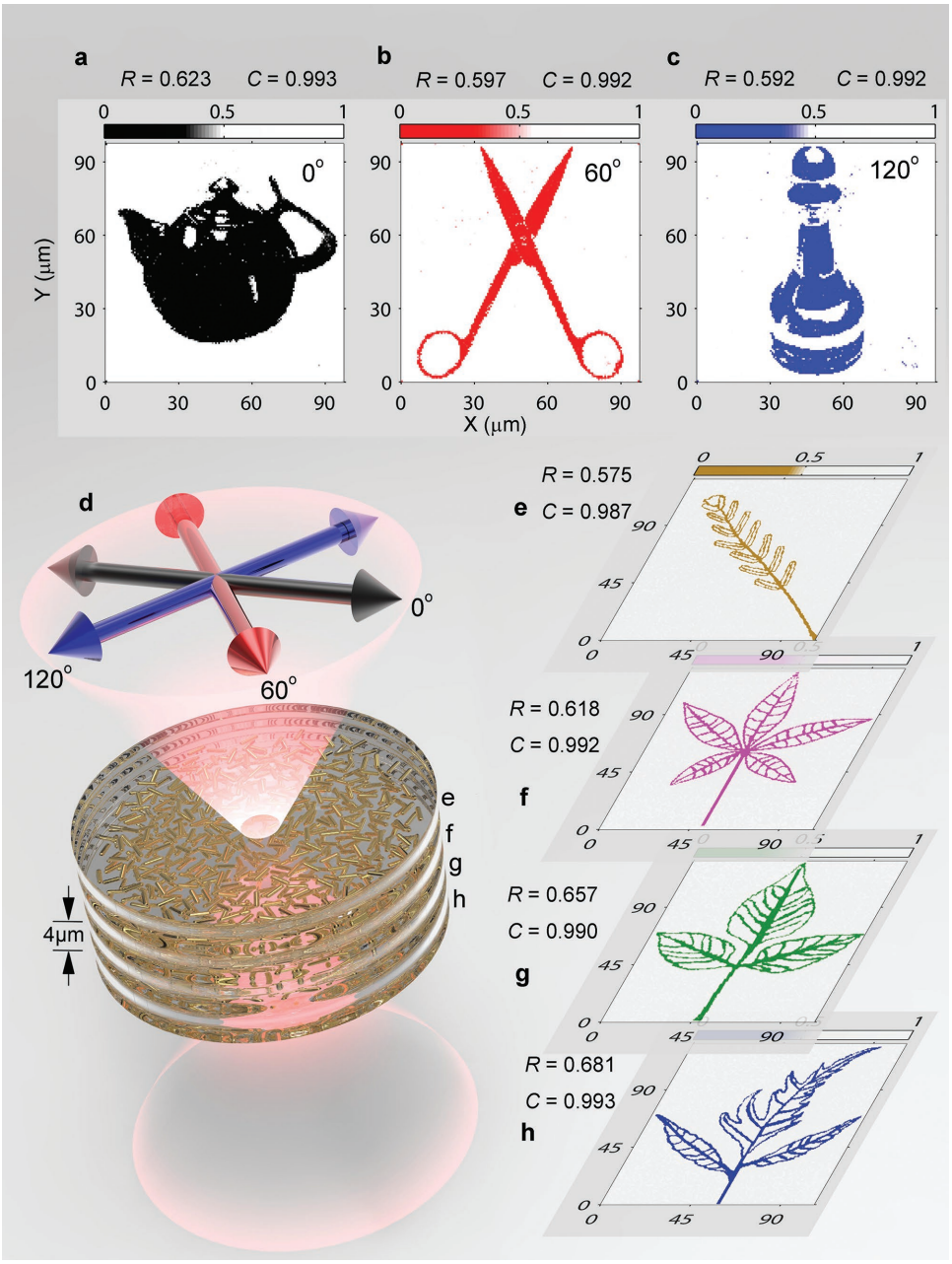


**Figure 4.** a–c) Patterns recorded and extracted by using fs laser light at 800 nm with polarization angles of 0°, 60°, and 120°. The size of information units was 0.65 × 0.65 μm$^2$. The pulse energies (or fluences) used for data recording and readout were 3.29 and 0.53 pJ (0.20 and 0.033 mJ cm$^{-2}$), respectively. d) Schematics showing the polarization multiplexing at three polarization angles (a)–(c) by using 800 nm fs laser light. e–h) Recording and readout of four patterns by directly focusing 750 nm fs laser light on different storage layers separated by 4.0 μm in a GNR-PVA film. The size of information units was 0.65 × 0.65 μm$^2$. The pulse energies (or fluences) used for data recording and readout were 3.29 and 0.53 pJ (0.20 and 0.033 mJ cm$^{-2}$), respectively. Here, pseudo colors are used to represent the patterns extracted from different polarization angles and different layers.

based on their melting energies (Figure 5a). Once a pattern is recorded by melting the first group of GNRs with the lowest melting energy (red GNRs), it can be readily erased by irradiating the unused information units with the same energy. After that, the second pattern can be recorded through the melting of the second group of GNRs (violet GNRs) with an increased recording and readout energies. The similar process can be repeated until the storage medium is damaged by high recording energies (Figures S19 and S20, Supporting Information). Four rewriting processes without cross-talk were demonstrated (Figure 5b–e), implying the realization of the rewriting function, which is not available for uncoupled GNRs (Figure S21, Supporting Information), by exploiting the energy of the laser pulses. It was also demonstrated that the rewriting function is independent of the polarization and wavelength multiplexing (Figure S22, Supporting Information), leading to

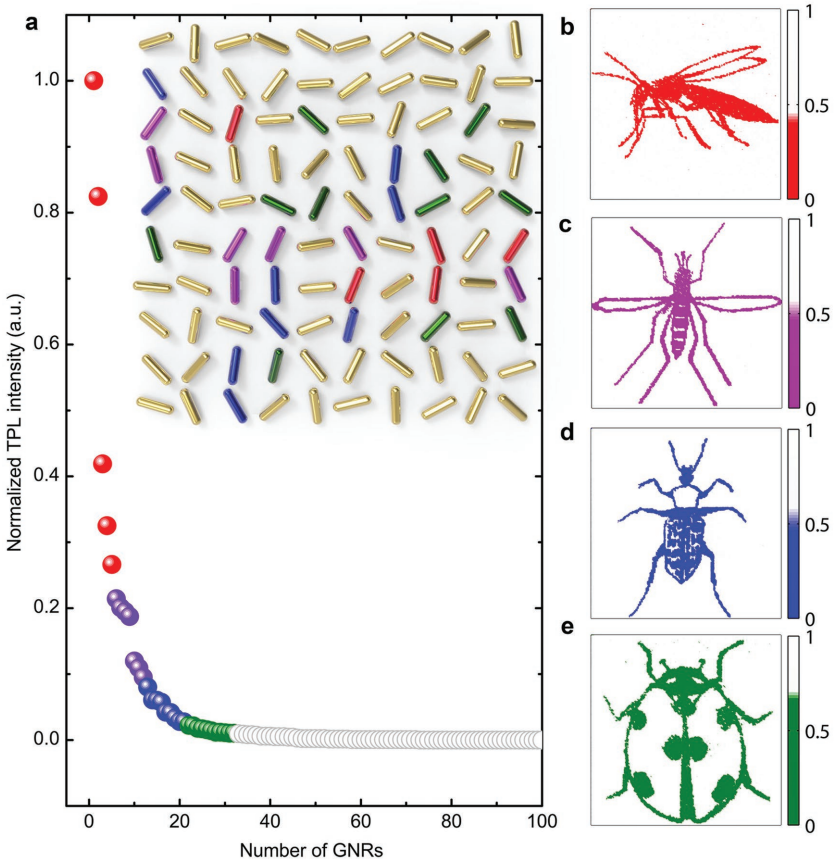


**Figure 5.** a) Distribution of the calculated TPL intensities of 100 GNRs in the GNR array with $S = 1L$ at an excitation wavelength of 1000 nm which is used to illustrate the principle of rewriting function. The GNRs in the array are classified into different groups based on their melting energies which are characterized by their TPA, as indicated by the colors (see also the inset). The melting of the GNRs in each group will lead to a contrast of ≈0.40. b–e) Four patterns recorded and extracted by using 750 nm fs laser light with different pulse energies. The size of information units was 0.65 × 0.65 μm$^2$. The pulse energies (or fluences) used for data recording and readout were (b) 3.16 and 0.42 pJ (0.19 and 0.026 mJ cm$^{-2}$), (c) 6.32 and 0.58 pJ (0.39 and 0.036 mJ cm$^{-2}$), (d) 17.37 and 0.84 pJ (1.07 and 0.052 mJ cm$^{-2}$), and (e) 34.21 and 1.32 pJ (2.10 and 0.081 mJ cm$^{-2}$). Here, pseudo colors are used to represent the patterns extracted from different rewriting processes.

a further enhancement in storage capacity. If we consider the use of four polarization channels and three wavelength channels, then the capacity of a DVD-sized disk will reach ≈20 TB (≈13.8 Tbit cm$^{-3}$) with rewriting four times, which indicates a significant progress in the multidimensional optical data storage based on GNRs.

In summary, we demonstrated a new concept for realizing ultrahigh-density optical data storage through the encoding of random hot spots induced by the plasmonic coupling between small GNRs, which significantly lowers the recording energy by two orders of magnitude and substantially improves the multiplexing function. We presented a numerical simulation whose results qualitatively agree with the experimental observations. The speed for data recording and readout can be significantly improved to gigabits per second by using the multifocal technology.[35] We anticipate that the demonstrated technology can facilitate the development of multidimensional optical data storage with ultrahigh density and ultralow energy.

## Experimental Section

*Sample Preparation*: GNRs with an average diameter of ≈8 nm and an average length of ≈34 nm were used to fabricate the storage media. They were synthesized by using a modified seedless method.[24] The polydispersity of GNRs was characterized by the linewidth of the longitudinal surface plasmon resonance which was derived from the absorption spectrum of the aqueous solution of GNRs. It was estimated to be ≈170 nm. The storage media were prepared by homogeneously dispersing GNRs in a 5% PVA solution and then spin-coating the solution on a glass cover slip. The thicknesses of the GNR-PVA films ranged from several to more than 20 μm, depending on the coating speed. The coupling strength between GNRs was controlled by adjusting the volume density of GNRs and it depends weakly on the length (or aspect ratio) of GNRs (Figure S23, Supporting Information). The concentrations of GNRs in the GNR-PVA films ranged from 330 ± 10 to 5280 ± 10 × 10$^{-9}$ M, corresponding to volume densities of 200–3200 GNR μm$^{-3}$. The photos for the fabricated GNR-PVA films can be found in Figure S10b (Supporting Information).

*Experimental Setup*: For optical data recording and readout, the fs laser light delivered by a Ti:sapphire oscillator (Mira 900S, Coherent) with duration of ≈130 fs and repetition rate of 76 MHz was focused on the storage medium by using the 60× objective (NA = 0.85) of an inverted microscope (Observer A1, Zeiss). The diameter of the laser spot was estimated to be ≈1.44 μm. The storage medium was placed on a 3D positioning system (P-563.3CD, Physik Instruments) with an accuracy of 1 nm in all dimensions. The fs laser light was fixed while the storage medium was moved by the positioning system. The TPL generated by the storage medium was collected by using the same objective and directed to a spectrometer (SR500i-B1, Andor) equipped with a photomultiplier tube (H7244-40, Hamamatsu) for analysis. The output signals from the photomultiplier tube were directed to a data acquisition system (BNC-2120, NI) after passing through a lock-in amplifier (SR850, Standford). A combination of a half-wavelength plate and a quarter-wavelength plate was employed to adjust the polarization of the fs laser light in the plane of the storage medium. A mechanical shutter was used to control the exposure time of the fs laser light during the processes of data recording and readout. For each information unit, the time for data recording and readout was set to be 20 ms which can be reduced by replacing the mechanical shutter with an acousto-optic modulator. A software was developed to control the synchronous operation of the mechanical shutter, the positioning system, and the data acquisition system. A pattern that had been recorded in the storage medium could be extracted by setting appropriate threshold intensity in the data readout process.

*Numerical Modeling*: The FDTD method (commercial software developed by Lumerical Solutions, Inc. (http://www.lumerical.com)) was employed to study the effects of hot spots on the linear and nonlinear optical properties of GNRs. The physical model used is a GNR array composed of 10 × 10 GNRs arranged on a square lattice with a lattice constant of $S$. For simplicity, all the GNRs are assumed to have the same length of $L = 25$ nm and the same diameter of $D = 6$ nm. The orientation of each GNR, which is characterized by two direction angles ($\Psi$ and $\theta$), is chosen to be a uniform random distribution within these ranges $0° < \Psi < 180°$ and $70° < \theta < 110°$ because GNRs with small and large $\theta$

are rarely observed in the storage media. The coupling strength between GNRs was adjusted by changing the lattice constant *S*. Different random realizations were checked and it was confirmed that the assumptions made above do not influence the main conclusions drawn in this work.

The calculation domain is about $1.35 \times 1.35 \times 0.10$ $\mu m^3$ and a nonuniform grid was applied with the smallest grid of 0.5 nm. Perfectly matched layers were applied to terminate the simulation domain. Total-field and scattered-field light sources were used to facilitate the calculation of the linear and nonlinear absorption of GNRs. The linear absorption of a GNR at a certain wavelength is equal to the integration of $\kappa|E|^2$ over the volume of the GNR, where $\kappa$ is the imaginary part of the complex refractive index of gold. Thus, the linear absorption of a GNR array at a certain wavelength can be derived by summing up the linear absorption of all the GNRs in the array. The TPA of a GNR is proportional to the integration of $|E|^4$ over the volume of the GNR and the total TPA of a GNR array can be obtained by summing up the contributions of all the GNRs, as established previously.[31–33] Since the TPL of a GNR is proportional to its TPA through a factor called quantum efficiency ($\eta$), TPA and TPL were not discriminated in the cases when only the relative intensities of them are concerned. The melting of a GNR was modeled by transforming it into a nanosphere with the same volume.

## Supporting Information

Supporting Information is available from the Wiley Online Library or from the author.

## Acknowledgements

S.L. thanks the financial support from the National Key Research and Development Program of China (No. 2016YFA0201002). S.L., Y.X. and Q.D. acknowledge the financial support from the National Natural Science Foundation of China (Grant Nos. 11374109, 11304047, and 60908040). S.L., Q.D., and S.T. would like to thank the financial support from the Natural Science Foundation of Guangdong Province, China (Grant Nos. 2016A030308010 and 2016A030313851) and that from the Science and Technology Planning Project of Guangdong Province, China (Grant No. 2015B090927006). Q.D. thanks the financial support from the Guangzhou Science and Technology Project (Grant No. 2011J2200080). M.G. thanks the Australian Research Council for its support through the Laureate Fellowship scheme (FL100100099) and the Centre of Excellence for Ultrahigh-bandwidth Devices for Optical Systems (CUDOS) (Project No. CE110001018).

## Conflict of Interest

The authors declare no conflict of interest.

## Keywords

gold nanorods, optical data storage, plasmonic coupling, random hot spots

Received: April 6, 2017
Revised: May 10, 2017
Published online:

[1] M. Gu, X. Li, Y. Cao, *Light: Sci. Appl.* **2014**, *3*, e117.
[2] B. Gjonaj, J. Aulbach, P. M. Johnson, A. P. Mosk, L. Kuipers, A. Lagendijk, *Nat. Photonics* **2011**, *5*, 360.
[3] S. Kawata, Y. Inouye, P. Verma, *Nat. Photonics* **2009**, *3*, 388.
[4] C. Clavero, *Nat. Photonics* **2014**, *8*, 95.
[5] P. Zijlstra, J. W. M. Chon, M. Gu, *Opt. Express* **2007**, *15*, 12151.
[6] P. Zijlstra, J. W. M. Chon, M. Gu, *Nature* **2009**, *459*, 410.
[7] X. Li, T. H. Lan, C. H. Tien, M. Gu, *Nat. Commun.* **2012**, *3*, 998.
[8] H. Ditlbacher, J. R. Krenn, B. Lamprecht, A. Leitner, F. R. Aussenegg, *Opt. Lett.* **2000**, *25*, 563.
[9] O. Wilson, G. J. Wilson, P. Mulvaney, *Adv. Mater.* **2002**, *14*, 1000.
[10] J. W. M. Chon, C. Bullen, P. Zijlstra, M. Gu, *Adv. Funct. Mater.* **2007**, *17*, 875.
[11] K. Choi, P. Zijlstra, J. W. M. Chon, M. Gu, *Adv. Funct. Mater.* **2008**, *18*, 2237.
[12] W. L. Leong, P. S. Lee, A. Lohani, Y. M. Lam, T. Chen, S. Zhang, A. Dodabalapur, S. G. Mhaisalkar, *Adv. Mater.* **2008**, *20*, 2325.
[13] D. Wan, H. L. Chen, S. C. Tseng, L. A. Wang, Y. P. Chen, *ACS Nano* **2010**, *4*, 165.
[14] A. Royon, K. Bourhis, M. Bellec, G. Papon, B. Bousquet, Y. Deshayes, T. Cardinal, L. Canioni, *Adv. Mater.* **2010**, *22*, 5282.
[15] A. Stalmashonak, A. Abdolvand, G. Seifert, *Appl. Phys. Lett.* **2011**, *99*, 201904.
[16] A. B. Taylor, J. Kim, J. W. M. Chon, *Opt. Express* **2012**, *20*, 5069.
[17] K. Grytsenko, O. Belyaev, A. Kryuchyn, I. Gorbov, S. Schrader, V. Ksianzou, *Opt. Memory Neural Networks* **2013**, *22*, 127.
[18] A. B. Taylor, P. Michaux, A. S. M. Mohsin, J. W. M. Chon, *Opt. Express* **2014**, *22*, 13243.
[19] L. Shao, K. C. Woo, H. Chen, Z. Jin, J. Wang, H. Lin, *ACS Nano* **2010**, *4*, 3053.
[20] L. S. Slaughter, Y. P. Wu, B. A. Willingham, P. Nordlander, S. Link, *ACS Nano* **2010**, *4*, 4657.
[21] M. D. Wissert, K. S. Ilin, M. Siegel, U. Lemmer, H. J. Eisler, *Nano Lett.* **2010**, *10*, 4161.
[22] W. Chen, F. Lin, Y. Lee, F. Li, Y. Chang, J. Huang, *ACS Nano* **2014**, *8*, 9053.
[23] Z. Huang, Q. Dai, S. Lan, S. Tie, *Plasmonics* **2014**, *9*, 1491.
[24] M. R. K. Ali, B. Snyder, M. A. El-Sayed, *Langmuir* **2012**, *28*, 9807.
[25] S. Link, M. A. El-Sayed, *J. Chem. Phys.* **2001**, *114*, 2362.
[26] F. Ercolessi, W. Andreoni, E. Tosatti, *Phys. Rev. Lett.* **1991**, *66*, 911.
[27] H. Chen, L. Shao, T. Ming, Z. Sun, C. Zhao, B. Yang, J. Wang, *Small* **2010**, *6*, 2272.
[28] H. D. Deng, G. C. Li, Q. F. Dai, M. Ouyang, S. Lan, V. A. Trofimov, T. M. Lysak, *Nanotechnology* **2013**, *24*, 075201.
[29] L. Cavigli, M. de Angelis, F. Ratto, P. Matteini, F. Rossi, S. Centi, F. Fusi, R. Pini, *J. Phys. Chem. C* **2014**, *118*, 16140.
[30] P. Zijlstra, J. W. M. Chon, M. Gu, *Phys. Chem. Chem. Phys.* **2009**, *11*, 5915.
[31] P. Ghenuche, S. Cherukulappurath, T. H. Taminiau, N. F. van Hulst, R. Quidant, *Phys. Rev. Lett.* **2008**, *101*, 116805.
[32] S. Viarbitskaya, A. Teulle, R. Marty, J. Sharma, C. Girard, A. Arbouet, E. Dujardin, *Nat. Mater.* **2013**, *12*, 426.
[33] L. Chen, G.-C. Li, G.-Y. Liu, Q.-F. Dai, S. Lan, S.-L. Tie, H.-D. Deng, *J. Phys. Chem. C* **2013**, *117*, 20146.
[34] H. Wang, T. B. Huff, D. A. Zweifel, W. He, P. S. Low, A. Wei, J.-X. Cheng, *Proc. Natl. Acad. Sci. USA* **2005**, *102*, 15752.
[35] X. Li, Y. Cao, N. Tian, L. Fu, M. Gu, *Optica* **2015**, *2*, 567.

 